1D and 2D FT-EPR Studies on the Photoinduced Electron Transfer Reaction from Zn Porphyrin to Duroquinone in CTAC Micellar Solution

Ryuji Hanaishi, Yasunori Ohba, Seigo Yamauchi,* and Masamoto Iwaizumi

Institute for Chemical Reaction Science, Tohoku University, Katahira 2-1-1, Aoba-ku, Sendai 980

(Received December 22, 1995)

A photoinduced electron transfer reaction in a model system of the photosynthesis was investigated by means of pulsed EPR in one (1D)- and two-dimensions (2D). EPR spectra of a spin correlated radical ion pair(SCRP) and a spin polarized radical anion were observed in the system of tetrakis(4-sulfonatophenyl) porphyrinozinc(II) (ZnTPPS)/duroquinone (DQ)/cetyltrimethylammonium chloride micellar solution. In order to investigate the dynamics and structures of the intermediate species, a non-linear least square fitting (NLLSQ), instead of linear prediction (LP), was examined for analyses of free induction decays (FID's) in a 1D experiment. FID's were fairly well reproduced with the NLLSQ method as a sum of the signals of the DQ anion and the SCRP. For the DQ anion, the linewidth gradually decreased indicating movement of the anion across the micelle/water interface.

For a definitive assignment of the SCRP, a 2D nutation experiment was performed. Different flip angle dependences were observed for the SCRP and the free anion. Under an assumption of an average exchange interaction (J), the 2D spectra of the SCRP were simulated, including an off-resonance effect on the basis of density matrix formalism. Comparison of the calculated and observed spectra indicated that the upper limit of the average $|J|$ was 0.3 MHz ($J < 0$).

Fourier-transform (FT) EPR spectroscopy has attracted much attention during the last decade.[1] A number of chemists have applied this technique to studies of photo-chemical reactions with an aid of high time resolution of 10 ns.[2] Several studies on spin dynamics of paramagnetic intermediates have also been reported with a two-dimensional (2D) FT-EPR technique.[3] However, there exist only a few examples where photochemical reactions are investigated by both the 1D and 2D FT-EPR techniques.[4] Recently, we have demonstrated the great abilities of 2D FT-EPR nutation spectroscopy in the study of a photochemically generated spin correlated radical pair (SCRP).[5] Some spectroscopic evidence for the spin-Hamiltonian and for a non-equilibrated spin polarization were found in the 2D spectra by observing flip angle dependence of the FT-EPR signal.

It is well known that a lifetime of SCRP drastically increases in viscous or micellar solution owing to restricted diffusion.[6,7] In this paper, we describe 1D and 2D FT-EPR studies of the SCRP and the free radical generated in the photoinduced electron transfer reaction from water-soluble tetrakis(4-sulfonatophenyl) porphyrinozinc(II) (ZnTPPS) to duroquinone (DQ) in the cetyltrimethylammonium chloride (CTAC) micellar solution. Recently van Willigen et al.[8] have studied 1D FT-EPR of this system and observed that the spectrum of the SCRP ([$ZnTPPS^{+}\cdots DQ^{-}$]) has a rather broad linewidth. They adopted the linear prediction (LP) SVD method[9] and the VARPRO routine[10] in order to reconstruct the part of FID lost during instrumental deadtime. An important point is that their spectra were reproduced as a sum of dispersive components of the peaks. This is unusual for the signal of long lived SCRP, which is the case of this system.[6,7]

This consideration has encouraged us to analyze the 1D FID by means of an another method, the non-linear least square (NLLSQ) fitting. The analyses would provide dynamic and structural information of the SCRP as well as those of the free radical, such as delay time dependences of an exchange J value, concentrations of the species, spin polarizations, and linewidths.

In the 2D experiment, we intended to demonstrate clearly a difference in the flip angle dependences between the SCRP and the free radical that was suggested by Kroll et al.[11] In a previous study of acetone in 2-propanol,[5] the signals of a radical and of a SCRP were mixed heavily, so the spectra were not completely separated. With an aid of preferentical dominance of the SCRP in this system, the 2D spectrum demonstrates the nutation frequency of the SCRP more distinctly than that reported for the acetone system. We also calculated the 2D nutation spectrum by using the density matrix method. From a comparison of experimentally obtained spectra with simulated ones, we obtained $|J| \leq 0.3$ MHz ($J < 0$). It was also found that both the 1D and 2D experiments provide consistent results for the J value.

Experimental and Data Processing

ZnTPPS was prepared from H_2TPPS (Strum) and zinc acetate hydrate (Wako Chemicals) and was purified following the reported procedure.[8] DQ and CTAC were used as received from Wako Chemicals. An aggregation number of 105 at a critical micelle concentration of 1.4 mM of CATC (1 M = 1 mol dm^{-3}) in water[8] was taken into account in preparation of aqueous solution, giving a micellar concentration of about 1 mM. The concentrations of

ZnTPPS and DQ were 0.4 and 2 mM, respectively. The solution was thoroughly deaerated by several freeze-pump-thaw cycles on a high-vacuum line and was sealed in a Pyrex® tube with outer diameter of 3 mm for the pulsed EPR measurement and of 1 mm for the continuous microwave (cw) time-resolved EPR (TREPR) measurement. The sample solution was sonicated during preparation and immediately before the measurements.

X-Band pulsed EPR experiments were performed with a Bruker ESP-380E spectrometer at room temperature. ZnTPPS was excited with the second harmonics (532 nm) of a Spectra Physics Quanta-Ray GCR-14S Nd : YAG laser with a repetition rate of 10 Hz. For 1D and 2D pulsed EPR experiments, the microwave (MW) pulse was synchronized to the laser pulse. Quadrature FID signals were accumulated with a LeCroy 9450A digital oscilloscope in a step of 10 ns by 512 steps. A duration of the MW pulse was ca. 10 ns in the 1D experiment. The delay time τ_d of the MW pulse from the laser excitation varied with a range from 100 ns to 10 μs. A quadrature detection of FID was completed with a four-step CYCLOPS phase cycling.

2D nutation spectra were observed at two different delay times, 1 μs and 10 μs, after the laser excitation. The duration of the MW pulse, t_1, increased in a step of 8 ns by 64 steps (8—512 ns), and FID (t_2) was collected in a step of 10 ns by 128 steps with the CYCLPOS phase cycling routine. Without extrapolation of the part of FID lost during the deadtime (ca. 88 ns), complex 2D FID of a matrix of 64×128 was apodized with the Hanning window in both dimensions (t_1 and t_2) and was zero-filled to 256×512. Then 2D complex fast Fourier transformation was applied to the 2D FID, $s(t_1, t_2)$, providing a 2D nutation spectrum $I(\omega_1,\omega_2)$, where ω_1 and ω_2 are a nutation frequency and an EPR frequency, respectively.

X-band cw-TREPR spectra were obtained with a NF BX-531 boxcar integrator as already described elsewhere.[12] The sample was excited with a Spectra Physics GCR170-10 Nd : YAG laser at 532 nm.

Results and Discussion

1D Experiments. 1. Spin-Correlated Radical Pair. The most simple technique of frequency analyses of FID is Fourier transformation. In FT-EPR measurements, the part of FID lost during instrumental deadtime causes distortion on a baseline of the FT spectrum. In order to extrapolate the missing part, the LP routine has been generally used for many cases. Here we examine the validity of this method.

We have observed 1DFT-EPR spectra in the system of ZnTPPS/DQ in CTAC micellar solution at room temperature, as shown in Fig. 1. These spectra were obtained with the LP method of LPQRD[13] and the fast LP routines[14] after reconstruction of the missing part of the FID. Similar spectra have already been reported by Levestein and van Willigen with the LPSVD method.[8] The observed signals are easily able to be assigned as those of the SCRP between $ZnTPPS^+$ and DQ^-.[6,7,15] From theories of the SCRP,[7] each hyperfine line of the signal could be analyzed by two in-phase(absorptive) components of opposite polarizations (*E/A*). Here *E/A* denotes to an emission and an absorption of microwave for the lower field and higher field components, respectively. It is, however, found from the LP solution that every peak was analyzed as a single line of an out-of-phase (dispersive) component. Such a dispersive component is expected to be

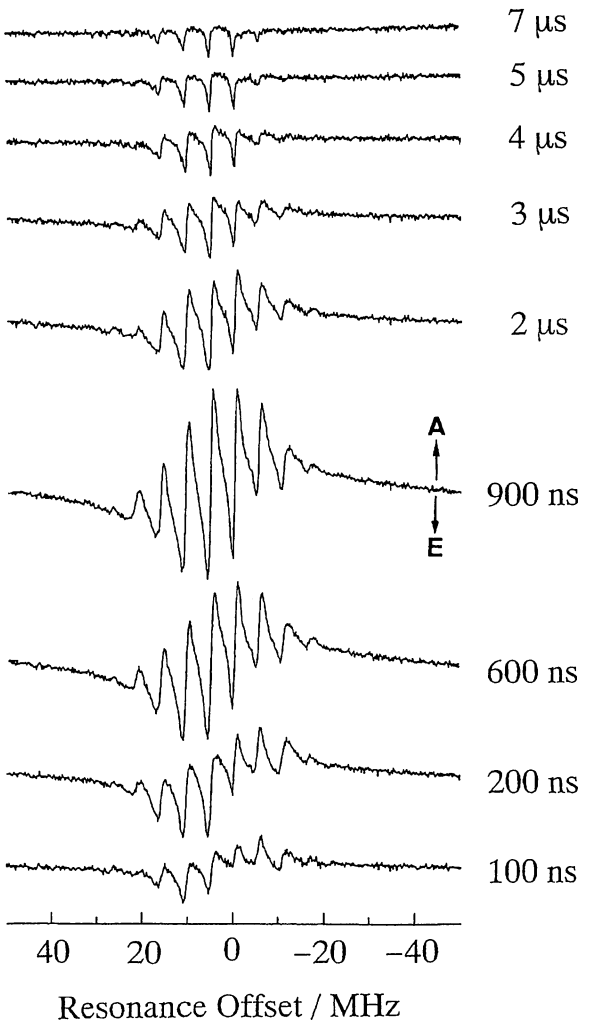

Fig. 1. 1D FT-EPR spectra of ZnTPPS/DQ/CTAC micellar solution with different delay time τ_d after reconstruction of lost parts of FID's with the LP solution.

observed for the FID of a radical affected by the short-lived SCRP. In our case, the SCRP is actually alive even at 2 μs, which is supported by an observation of a cw-TREPR spectrum (Fig. 2d).

In order to clarify the difference between absorptive and dispersive spectra, we compare three kinds of FT-FID spectra with the cw-TREPR spectra in Fig. 2: Spectrum (a) was simulated with the LP solution of the observed FID. Spectrum (b) is a simulation spectrum under an assumption of (absorptive) *E/A* peaks with an appropriate J (−0.3 MHz) and a linewidth Γ (1 MHz), and spectrum (c) is the same one as shown in Fig. 1. Spectrum (d) shows the TREPR spectrum observed at 2 μs after the laser pulse. We consider that the cw-TREPR spectrum reflects a real lineshape of the SCRP spectrum. From these spectra, it is found that the spectrum with LP roots (a) is composed of all dispersive components which are characterized by very broad lines at both wings of the spectrum. Spectrum (b) with absorptive *E/A* resembles the TREPR spectrum closely. Spectrum (c) obtained from

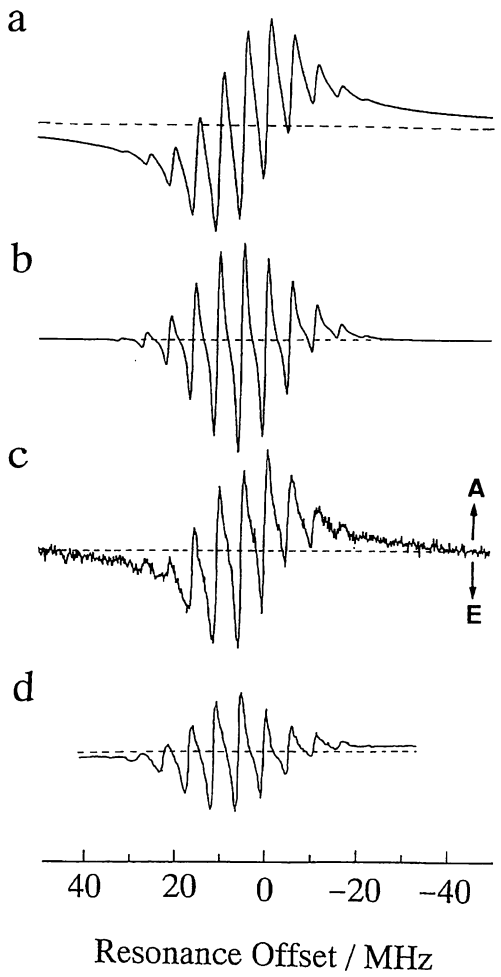

Fig. 2. Three different types of 1D FT-EPR spectra with delay time τ_d of 2 μs; (a) a simulated spectrum based upon the LP solution of FID, (b) a simulated spectrum obtained for *E/A* peaks with single *J* of −0.3 MHz, and (c) a spectrum obtained after extrapolation with the LP solution. (d) shows a cw TR-EPR spectrum observed at 2 μs with a gate width of 0.2 μs.

the observed and reconstructed FID is an intermediate one between (a) and (b) showing still broad components. We also found that the given *E/A* components (b) are analyzed with the LP method as dispersive components by suffering similar noise to that of the observed FID. These observations clearly indicate that two lines of closely separated *E/A* components can not be correctly resolved by the LP method under ordinary conditions. The most serious problem of the LP analysis giving dispersive components is that neither *J* nor Γ can be determined in many cases.

Therefore, we next examined the non-linear least square (NLLSQ) fitting of FID with a model containing an absorptive anti-phase (*E/A*) doublet. First, we point out that the spectrum of the $ZnTPPS^+$ radical is broadened inhomogeneously with very short T_2^*[8] and the FID contains very few contributions from this radical after the instrumental dead-time (88 ns). We here consider only the EPR transitions due to the SCRP of the DQ anion radical. For hyperfine peaks of M_I, the FID is described as

$$\begin{aligned} s(M_I,t) &= n(M_I)[\exp\{2\pi i(f(M_I)-J)t - 2\pi\Gamma t + i\phi(M_I)\} \\ &\quad - \exp\{2\pi i(f(M_I)+J)t - 2\pi\Gamma t + i\phi(M_I)\}] \\ &= 2n(M_I)[\sin(2\pi Jt)[\sin\{2\pi f(M_I)t + \phi(M_I)\} \\ &\quad - i\cos\{2\pi f((M_I)t + \phi(M_I)\}]\exp\{-2\pi\Gamma t\}, \end{aligned} \quad (1)$$

where the transverse magnetization damps exponentially with Γ, Here, $n(M_I)$ is the number of degenerate nuclear configurations, $f(M_I)$ a resonance offset at M_I, *J* an average exchange coupling constant, Γ a linewidth, $\phi(M_I)$ an initial phase. By summing up contributions from all hyperfine lines, the whole FID is described as

$$s(t) = A\sum_{M_I} s(M_I,t), \quad (2)$$

with an amplitude factor of *A*.

First we examined dependences of the linewidth Γ and the exchange integral *J* in a 2D fashion. The Γ and $|J|$ values altered over 0.05—10 MHz in 0.05 MHz steps. It turns out that the Γ which minimizes the difference between the observed and calculated FID's had a range from 0.8 to 1.0 MHz. The obtained *J*'s were summarized in Fig. 3, including error bars. Next, by using these Γ and *J* values as initial values we made the NLLSQ fitting of the observed FID with the algorithm of Marquardt, involving the method of Taylor's differential correction.[16] Here *J*, Γ, and *A* are non-linear parameters. We used fixed values for $f(M_1)$ and $\phi(M_I)$ obtained from the LP solution. The Γ values which minimize the residues are listed in Table 1 and the plots of the *J* value vs. delay time τ_d are shown in Fig. 3. Contrary to the previous report,[8] no notable dependence of the linewidth on the hyperfine lines was observed. It seems that the reported linewidths contained appreciable errors due to the aforementioned misunderstanding

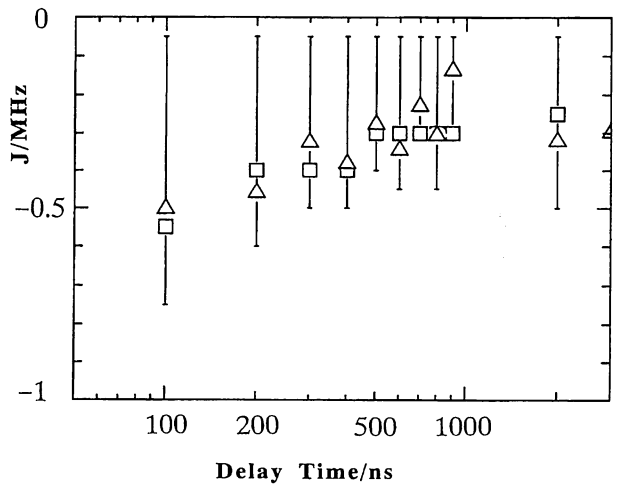

Fig. 3. Plots of obtained exchange coupling *J* versus delay time τ_d. Squares express the most suitable *J* values when *J* and Γ varied in a 2D fashion. Error bars denote the ranges where the residue does not exceed over the minimal one by a factor of 1%. Triangles express the converged *J* values when the NLLSQ fitting was applied. See the text.

Table 1. Most Suitable Linewidth Γ at Different Delay Time τ_d[a)]

τ_d/ns	100	200	300	400	500	600	700	800	900	2000	3000
Γ/MHz	0.82	0.79	0.93	0.87	0.93	0.88	0.95	0.91	0.96	0.86	0.88

a) Values were obtained by the Marquardt NLLSQ fitting of the FID.

of the line-shape.

Although the shape of the FID was not so sensitive to J in its small region, we found that the absolute value of $|J|$ gradually decreases with the delay time. This result may be explained in terms of relative diffusion of the pair after the electron transfer reaction. Another possible reason is that a spin relaxation prefers the group of the pairs with larger $|J|$ values compared to those with small $|J|$'s.

The time dependence of the obtained A value on τ_d could provide dynamics of the SCRP as shown in Fig. 4. We assumed the first order rise and decay of the signal; then time constants were obtained as 3×10^6 s^{-1} and 4×10^5 s^{-1}, respectively. These values are consistent with the reported ones,[8)] which also assures reliability of the NLLSQ analyses. Then, the reaction scheme is summarized as the following.

$$\mathrm{ZnTPPS} \xrightarrow{h\nu} {}^3\mathrm{ZnTPPS}^* \xrightarrow[3\times10^6\ \mathrm{s}^{-1}]{\mathrm{DQ}} \underset{\mathrm{SCRP}}{[\mathrm{ZnTPPS}^+\cdots\mathrm{DQ}^-]} \xrightarrow[4\times10^5\ \mathrm{s}^{-1}]{} \underset{\text{free radicals}}{\mathrm{ZnTPPS}^+ + \mathrm{DQ}^-}$$

The observed FID, the calculated FID with the given parameters (Table 1, Figs. 3 and 4), and the residues are shown in Fig. 5 for both the real and imaginary parts.

2. Free Radical. As shown in Fig. 1, we observed in-phase emissive signals after the delay time τ_d of 7 μs. These signals are safely attributed to those of isolated spin polarized DQ anion radical. The residues in Fig. 5, which are called "difference FID", contain contributions from the components other than the SCRP. Complex FT of this difference FID yields a "difference spectrum", where extrapolation of the lost part was not made. Although the spectra suffered from distortions in the baselines, we can evaluate the amplitudes and phases of the signals. The difference spectra at several delay times are shown in Fig. 6. The spectra did not show the anti-phase (E/A) doublet signals of the SCRP, but one phase (E or A) signal of the free radical involving CIDEP. Therefore, we conclude that the difference spectra come from the free DQ anion radical.

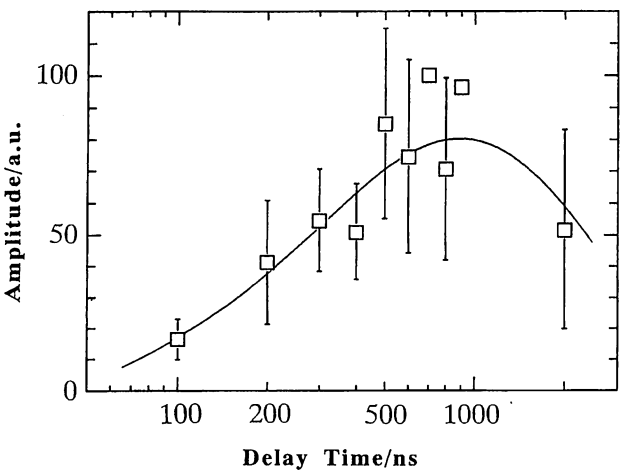

Fig. 4. Plots of amplitude factor A of the SCRP versus delay time τ_d. The value is directly proportional to the concentration of the SCRP.

The polarization of the spectrum varied with τ_d. Immediately after the laser pulse, the low field components exhibit a stronger emission (E) and the high field components an absorption (A) of the microwave, giving an E^*/A pattern. This polarization can be easily simulated by both contributions of the triplet mechanism (TM)[17)] due to polarized ZnTPPS* (A) and the ST_0 mixing (triplet precursor, $J<0$) in the radical pair mechanism (RPM)[18)] with E^*/A (Fig. 7a). Soon after the intensities of the high field lines were weakened, the polarizations were inverted to the emission. The whole emissive spectrum at 10 μs was shown in Fig. 7c. This emissive polarization can be attributed to either or both of the two possible mechanisms. One is the electron exchange between neutral DQ and the DQ anion.[8,9,20)] In this case, prevailing emissive polarizations produced by ST_0 RPM (E^*/A) are transferred from one hyperfine line to the other before the longitudinal relaxation is completed. Another possibility is the ST_- RPM[21)] (Fig. 7b). Taking into account the relatively strong E (Fig. 6a) signal vs the E^*/A (Fig. 6d) signal at earlier time and similarity of the spectra (Figs. 7b and 7c), we considered that the ST_- mechanism is involved in this system. The observation that emissive electron spin echo (ESE) signal of the $ZnTPPS^+$ radical was observed in this system[22)] together with those of the SCRP and the DQ anion radical is consistent with this assignment.

In the spectra of the DQ anion radical, the linewidth became narrower with increasing τ_d. Levstein and van Willigen observed similar behavior in micellar solution with a neutral surfactant of TX100, where the linewidth broadening was observed at a much earlier time ($\tau_d<40$ ns).[8)] In our case, however, the linewidth varied after ca. 1 μs. The change in the linewidth could be ascribed to movement of the DQ anion from the micelle/water interface to the bulk aqueous phase, where the interactions with the ZnTPPS radical and/or the cationic CTAC surfactant must be reduced.[8,23)] Coulomb interactions between the DQ anion and the positively charged heads of CTAC and/or electron exchanges between DQ^- and DQ may be concerned with the linewidth broadening inside the micelle (<1 μs).

2D Nutation Experiments. We obtained 2D spectra with respect to two frequency axes, a nutation frequency (ω_1) and an EPR frequency (ω_2). 2D nutation spectra are displayed at two different delay times: 1 μs, and 10 μs, in Fig. 8. Contour maps of these spectra are shown in Fig. 9.

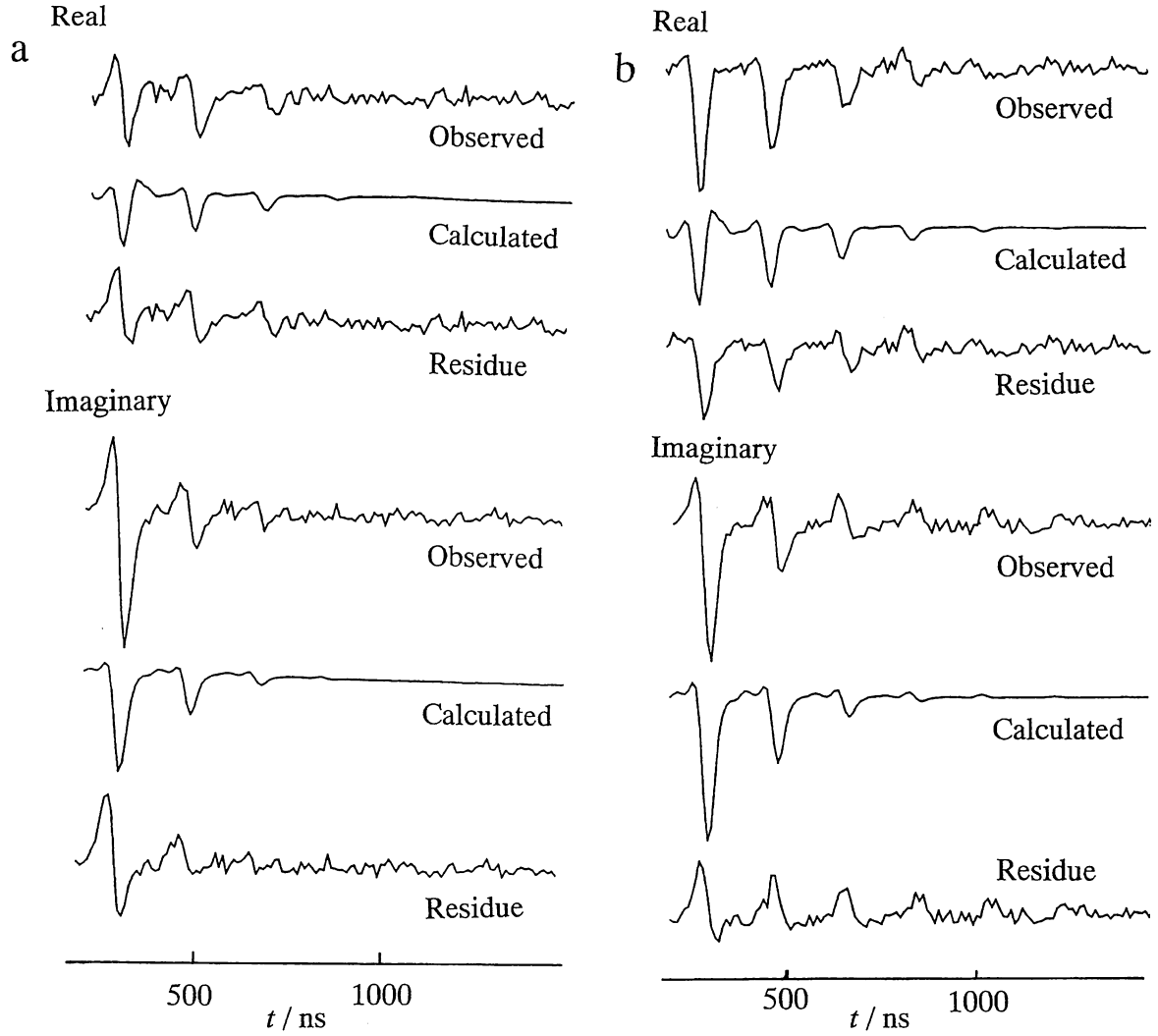

Fig. 5. Observed and the calculated FID's for the SCRP with the Marquardt routine and the residual FID at delay times of (a) 100 ns and (b) 3 μs for the real and the imaginary parts.

Comparison of the two spectra leads us to the conclusion that correlation between ω_1 and ω_2 in each peak is remarkably different at two delay times. As mentioned in the previous section, the 1D experiments reveal that the EPR signals comprise dominantly those of the SCRP at the delay time of 1 μs, whereas the free radical exclusively at 10 μs (Fig. 1). It is easily shown that only the Torrey oscillation for a two-level system[24] involved in the nutation spectrum (ω_1) at 10 μs; the spectrum is fairly well explained by the nutation of the longitudinal magnetization of the free radical[5] with a frequency $\omega_1/2\pi$ of ca. 12 MHz at the center of the spectrum ($\omega_2 \approx 0$ MHz). The nutation spectrum at 1 μs gave the maximum intensity at the nutation frequency $\omega_1/2\pi$ of ca. 28 MHz at $\omega_2 \approx 0$ MHz. This ω_1 value is about twice of that for the radical, which clearly indicates that the observed nutation spectrum (Fig. 8a) is due to that of the SCRP.[11,25] This assignment is also consistent with the result of the 1D experiment.

Next we try to simulate the 2D spectrum of the SCRP using the method of a density matrix. The averaged Hamiltonian theory provides time evolution of the density matrix in a rotating frame as[5]

$$\sigma(t_1,t_2) = \exp\{-iH_0t_2\}\exp\{-i(H_0+H_p)t_1\}\sigma(0)\exp\{i(H_0+H_p)t_1\} \times \exp\{iH_0t_2\}, \quad (3)$$

where $\sigma(0)$ expresses an initial density matrix, H_0 the spin Hamiltonian of the SCRP, H_p the Hamiltonian of an interaction with an alternating MW field. All the Hamiltonians are written in angular frequency units. t_1 and t_2 are evolution times with and without the MW field, respectively. In the above description, we ignored effects of spin relaxation and further development of a spin polarization and used an average J value during the evolution of the system. Under the high field approximation, the spin Hamiltonian of the SCRP is described as

$$H_0 = \Omega_a S_{az} + \Omega_b S_{bz} - J(2S_aS_b + 1/2), \quad (4)$$

where Ω_a and Ω_b are resonance offsets of radicals a and b, respectively. On the other hand, we have

$$H_p = -g_a\mu_B S_{ay}/\hbar - g_b\mu_B S_{by}/\hbar. \quad (5)$$

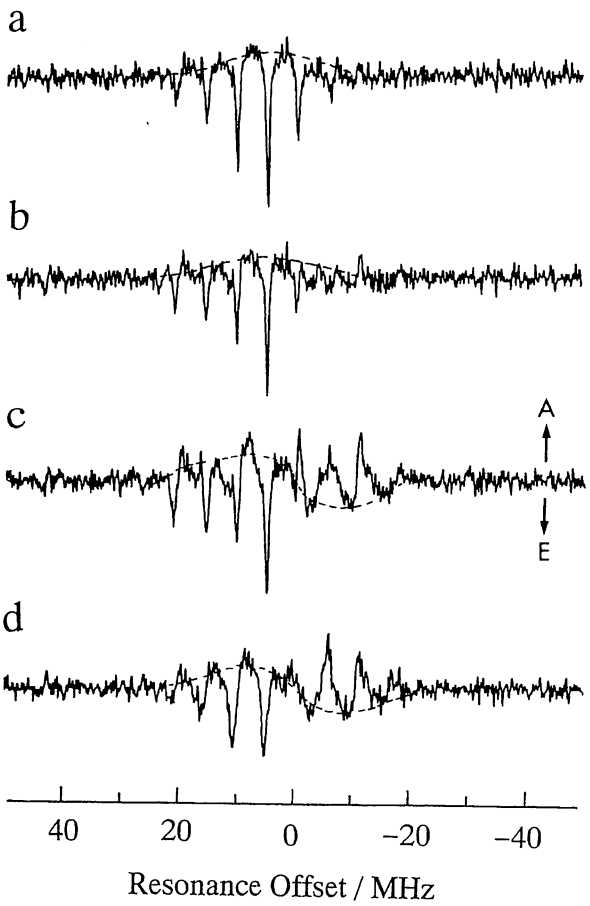

Fig. 6. Difference spectra at delay times τ_d of (a) 3 μs, (b) 2 μs, (c) 200 ns, and (d) 100 ns. These spectra were obtained by Fourier transformation of the residual FID (Fig. 4). Broken lines indicate approximate baselines.

Because of the short T_2^* of the $ZnTPPS^+$ radical,[8] the observed FID consists of contribution only from the DQ^- radical in the SCRP. In order to obtain magnetization of the DQ^- radical, one needs to calculate a trace of the spin density matrix over a subspace of the $ZnTPPS^+$ radical as follows:

$$\sigma_{DQ}(t_1,t_2) = tr_{ZnTPPS}\{\sigma(t_1,t_2)\}$$

$$= tr_{ZnTPPS}\left\{\begin{array}{c} \begin{matrix} \alpha\alpha & \alpha\beta & \beta\alpha & \beta\beta \end{matrix} \\ \left[\begin{matrix} \sigma_{\alpha\alpha\alpha\alpha} & \sigma_{\alpha\alpha\alpha\beta} & \sigma_{\alpha\alpha\beta\alpha} & \sigma_{\alpha\alpha\beta\beta} \\ \sigma_{\alpha\beta\alpha\alpha} & \sigma_{\alpha\beta\alpha\beta} & \sigma_{\alpha\beta\beta\alpha} & \sigma_{\alpha\beta\beta\beta} \\ \sigma_{\beta\alpha\alpha\alpha} & \sigma_{\beta\alpha\alpha\beta} & \sigma_{\beta\alpha\beta\alpha} & \sigma_{\beta\alpha\beta\beta} \\ \sigma_{\beta\beta\alpha\alpha} & \sigma_{\beta\beta\alpha\beta} & \sigma_{\beta\beta\beta\alpha} & \sigma_{\beta\beta\beta\beta} \end{matrix}\right] \end{array}\right\}$$

$$= \begin{array}{c} \begin{matrix} \alpha & \beta \end{matrix} \\ \left[\begin{matrix} \sigma_{\alpha\alpha\alpha\alpha} + \sigma_{\alpha\beta\alpha\beta} & \sigma_{\alpha\alpha\beta\alpha} + \sigma_{\alpha\beta\beta\beta} \\ \sigma_{\beta\alpha\alpha\alpha} + \sigma_{\beta\beta\alpha\beta} & \sigma_{\beta\alpha\beta\alpha} + \sigma_{\beta\beta\beta\beta} \end{matrix}\right] \end{array} . \quad (6)$$

Here in σ_{1234} (1,2,3,4=α or β), 1 and 3 denote electron spins of the DQ^- radical, and 2 and 4 denote electron spins of the $ZnTPPS^+$ radical. Hence, 2D FID of the SCRP from the DQ^- radical is expressed as

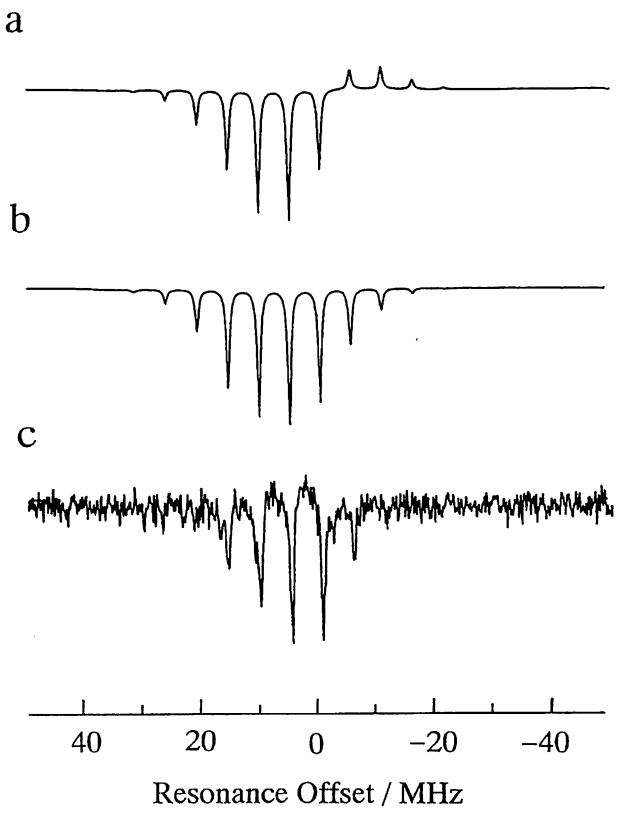

Fig. 7. Calculated spectra due to a) ST_0 and b) ST_- mechanisms with EPR parameters of $g(DQ^-)=2.0049$, $g(ZnTPPS^+)=2.0025$, $a(12H)=5.40$ MHz, and $a(4N)=4.30$ MHz, and c) the difference spectrum at 10 μs.

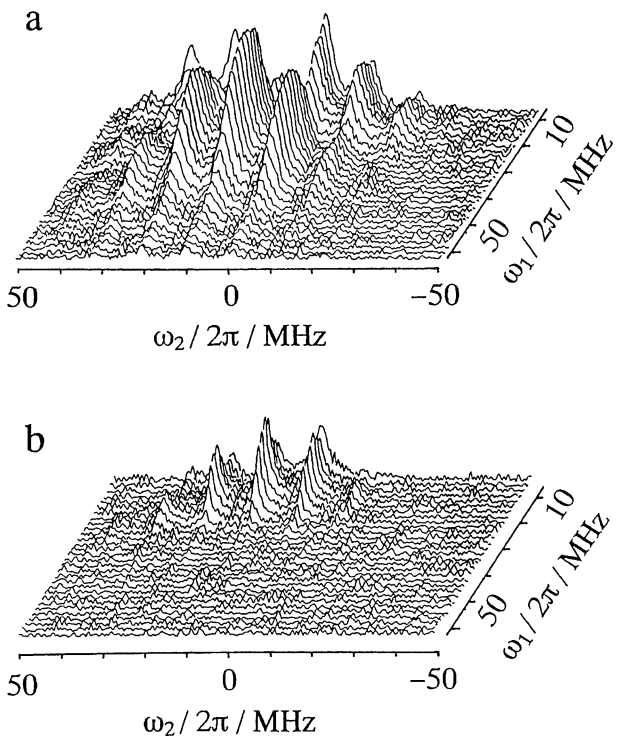

Fig. 8. 2D FT-EPR nutation spectra at delay times of (a) 1 μs and (b) 10 μs. ω_1 and ω_2 denote the nutation frequency and the EPR frequency, respectively.

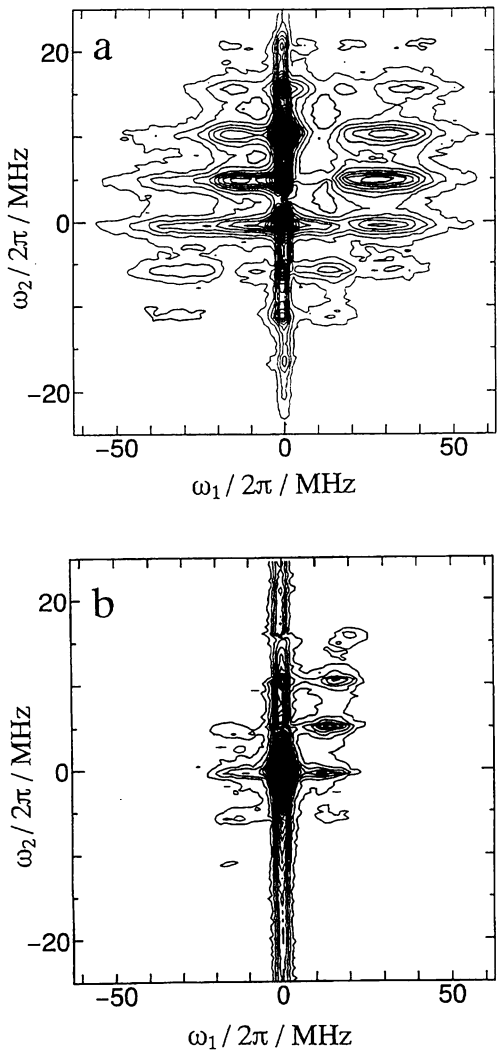

Fig. 9. Contour plots of Figs. 8(a) and 8(b). Note that the peaks with the higher nutation frequencies (ω_1) were observed in (a).

$$s(t_1,t_2) = tr\{(S_x + iS_y)\sigma_{DQ}(t_1,t_2)\} = \sigma_{\beta a a a}(t_1,t_2) + \sigma_{\beta\beta a\beta}(t_1,t_2). \quad (7)$$

Since a shape of the EPR spectrum of the $ZnTPPS^+$ radical can be approximated by the Gaussian lineshape with a full width at half maximum of ca. 16.5 MHz, we considered the spectrum as 11 lines separated by 4.0 MHz with the Gaussian distribution as shown in Fig. 10. Then the nutation spectrum is obtained by 2D Fourier transformation of Eq. 7 as

$$I(\omega_1,\omega_2) = \int_{-\infty}^{\infty}\int_{-\infty}^{\infty} dt_1 dt_2 e^{-i\omega t_1} e^{-i\omega t_2} s(t_1,t_2). \quad (8)$$

We calculated the 2D spectra using the parameters as summarized in Table 2 for several J values, as shown in Fig. 11. These figures unambiguously demonstrate that the observed spectra having the *E/A* patterns are due to those of the SCRP. All the spectra except the one with J of -1.0 MHz have lineshapes similar to each other. Therefore, we can conclude

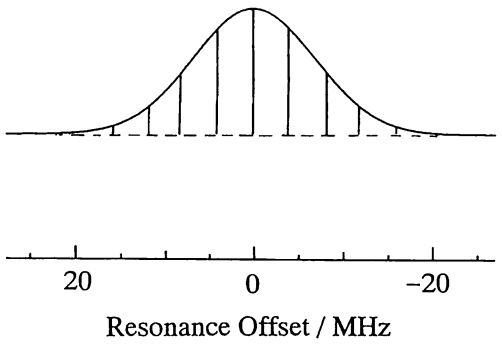

Fig. 10. A simplified spectrum of the $ZnTPPS^+$ radical used for the simulation of 2D spectra.

Table 2. Parameters Used for the Simulation of 2D Nutation Spectra Displayed in Fig. 11[1)]

Center of the spectrum of DQ	4.99 MHz
Center of the spectrum of ZnTPPS	−5.60 MHz
g(DQ)	2.0049
g(ZnTPPS)	2.0025
B_1	0.421 mT
a(DQ)	5.40 MHz

a) The spectrum of the $ZnTPPS^+$ radical is described in Fig. 10.

that the exchange interaction parameter $|J|$ ($J<0$) is smaller than ca. 0.3 MHz, which was also obtained from the 1D experiment. From our results it is found that the 1D and 2D FID's in micellar solution are satisfactorily simulated by a model of the average J value.[26)]

Conclusions

Dynamic and structural studies were made on the radical and spin correlated radical pair (SCRP) in the photoinduced electron transfer system of ZnTPPS/DQ/CTAC micellar solution by means of pulsed EPR in one (1D) and two (2D) dimensions.

In order to analyze the 1D FID of the SCRP as well as the DQ anion radical, we examined two kinds of analytical approaches. Application of the linear prediction (LP) method turned out to fail in the analyses, whereas the nonlinear least square (NLLSQ) fitting fairly well reproduced the obtained FID. We found that the J value of the SCRP gradually decreases with delay time τ_d. The difference in the observed and calculated FID's for the SCRP(difference FID) comprises the contribution from the free radical. The linewidth narrowing observed for the DQ^- radical indicates an escape of the anion from the micelle to bulk water solution at a later time.

Two-dimensional nutation experiments gave definitive evidence for the assignment of the SCRP. The obtained nutation spectra showed completely different features at different delay times when the SCRP exists and does not. From the numerical calculation of the 2D spectra we obtained the upper limit of the exchange value $|J|$. Both 1D and 2D nutation experiments provided almost the same $|J|$ value of ≤ 0.3 MHz ($J<0$).

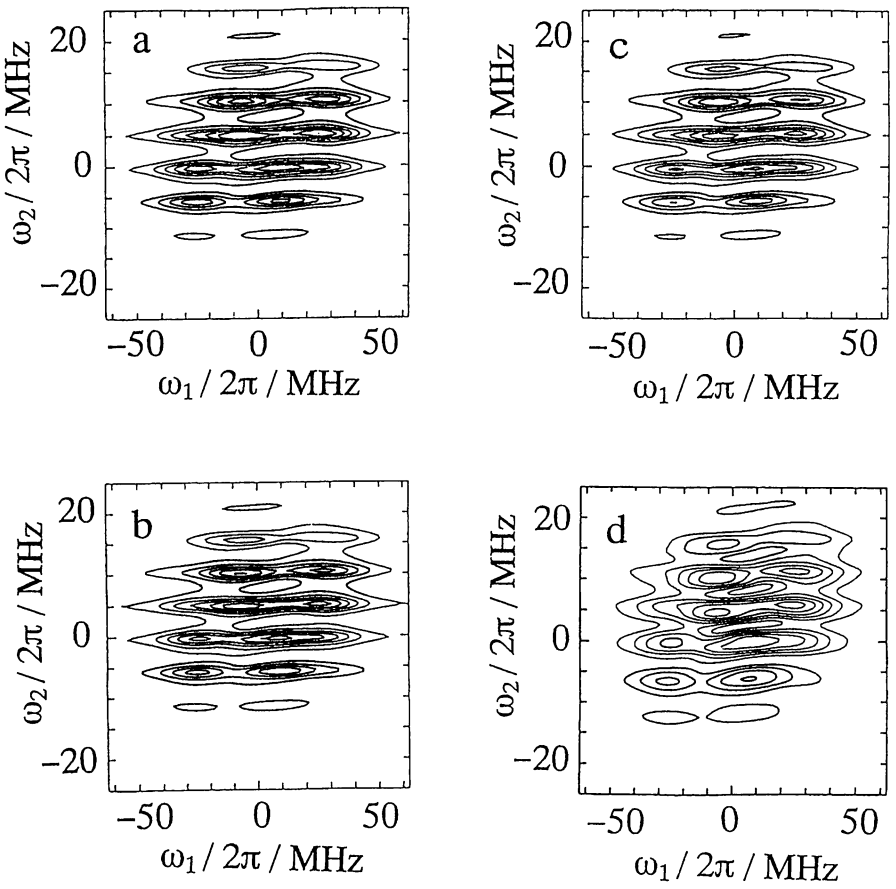

Fig. 11. Calculated 2D nutation spectra with four different J values of (a) −0.03 MHz, b) −0.1 MHz, (c) −0.3 MHz, and (d) −1 MHz. Other parameters are listed in Table 2.

Financial supports by Grants-in-Aid for Scientific Researches Nos. 06640711 (M. I.), 04242102 (S. Y.), and 06239208 (S. Y.) from the Ministry of Education, Science, Sports and Culture were essential to this work. The authors thank Prof. Kimio Akiyama of this institute for his help in the 2D-EPR measurements.

References

1) L. Kevan and M. K. Bowman, "Modern Pulsed and Continuous Wave Electron Spin Resonance," Wiley, New York (1990).

2) H. van Willigen, P. R. Levstein, and M. H. Ebersole, *Chem. Rev.*, **93**, 173 (1993), and references cited therein.

3) S. Lee and J. H. Freed, *J. Chem. Phys.*, **101**, 5529 (1994), and references cited therein.

4) M. Plüsuhau and K.-P. Dinse, *J. Magn. Reson., Ser. A*, **109**, 181 (1994).

5) R. Hanaishi, Y. Ohba, K. Akiyama, S. Yamauchi, and M. Iwaizumi, *J. Magn. Reson., Ser. A*, **116**, 196 (1995); *J. Chem. Phys.*, **103**, 4819 (1995).

6) a) S. Sakaguchi, H. Hayashi, H. Murai, and Y. J. I'haya, *Chem. Phys. Lett.*, **110**, 275 (1984); b) K. Tominaga, S. Yamauchi, and N. Hirota, *Chem. Phys. Lett.*, **149**, 32 (1988).

7) a) G. L. Closs, M. D. E. Forbes, and J. R. Norris, *J. Phys. Chem.*, **91**, 3592 (1987); b) C. D. Buckley, D. A. Hunter, P. J. Hore, and K. A. McLauchlan, *Chem. Phys. Lett.*, **135**, 307 (1987).

8) P. R. Levstein and H. van Willigen, *Chem. Phys. Lett.*, **187**, 415 (1991).

9) H. Barkhuysen, R. de Beer, W. M. M. J. Bovée, and D. van Ormondt, *J. Magn. Reson.*, **61**, 465 (1985).

10) G. H. Gloub and V. Pereyra, *SIAM J. Numer. Anal.*, **10**, 413 (1973).

11) G. Kroll, M. Plüshau, K.-P. Dinse, and H. van Willigen, *J. Chem. Phys.*, **93**, 8709 (1990).

12) S. Ohkoshi, S. Yamauchi, Y. Ohba, and M. Iwaizumi, *Chem. Phys. Lett.*, **224**, 313 (1994).

13) J. Tang, C. P. Lin, and J. R. Norris, *J. Magn. Reson.*, **62**, 167 (1985).

14) H. Gesmar and P. C. Hansen, *J. Magn. Reson., Ser. A*, **106**, 236 (1994).

15) M. C. Thurnauer, M. K. Bowman, and J. R. Norris, *FEBS Lett.*, **100**, 309 (1979).

16) D. W. Marquardt, *J. SIAM.*, **11**, 431 (1963).

17) S. K. Wang, D. A. Hutchinson, and J. K. Wan, *J. Chem. Phys.*, **58**, 985 (1973).

18) F. Adrian, *J. Chem. Phys.*, **53**, 3374 (1970).

19) P. R. Levstein, H. van Willigen, M. Ebersole, and F. W. Pijipers, *Mol. Cryst. Liq. Cryst.*, **194**, 123 (1991).

20) S. Basu, K. A. McLauchlan, and A. J. D. Ritchie, *Chem. Phys. Lett.*, **105**, 447 (1984).

21) a) F. J. Adrian and L. Monchick, *J. Phys. Chem.*, **71**, 2600 (1979); b) M. Terazima, Y. Miura, K. Ohara, and N. Hirota, *Chem. Phys. Lett.*, **224**, 95 (1994).

22) R. Hanaishi, K. Yamamoto, Y. Ohba, S. Yamauchi, and M. Iwaizumi, *Appl. Magn. Reson.*, in press.

23) K. M. Kadish, G. B. Maiya, and R. Guillard, *Inorg. Chem.*, **28**, 2725 (1989).
24) H. C. Torrey, *Phys. Rev.*, **76**, 1059 (1949).
25) K. Harasharoni, H. Levanon, J. Tang, M. K. Bowman, J. R. Norris, D. Gust, T. A. Moore, and A. L. Moore, *J. Am. Chem. Soc.*, **112**, 6477 (1990).
26) Very recently Tarasov et al. have examined the simulation of the SCRP spectrum including a time dependent J value and attached its importance.[27)]
27) V. F. Tarasov, E. G. Bagraynskaya, I. A. Shkrob, N. I. Avdievich, N. D. Ghatlia, N. N. Lukzen, N. N. Turro, and R. Z. Sagdeev, *J. Am. Chem. Soc.*, **117**, 110 (1995).